Supplementary Information

High-Performance Photodetector Enabled by Melamine Cation Based Lead Free Perovskitoid Single Crystals

Xin Yang,[a,b] Yu-Hua Huang,[a] Qiang-Sheng Zhang,[c] Xu-Dong Wang[a] and Dai-Bin Kuang*[a]*

[a]Key Laboratory of Bioinorganic and Synthetic Chemistry of Ministry of Education, LIFM, GBRCE for Functional Molecular Engineering, School of Chemistry, IGCME, Sun Yat-Sen University, Guangzhou 510275, China.

[b]School of Chemistry, Guangdong University of Petrochemical Technology, Maoming 525000, China.

[c]Hainan Provincial Key Laboratory of Fine Chem, School of Chemistry and Chemical Engineering, Hainan University, Haikou 570228, China.

E-mail: wangxd26@mail.sysu.edu.cn (X.-D. Wang); kuangdb@mail.sysu.edu.cn (D. B. Kuang)

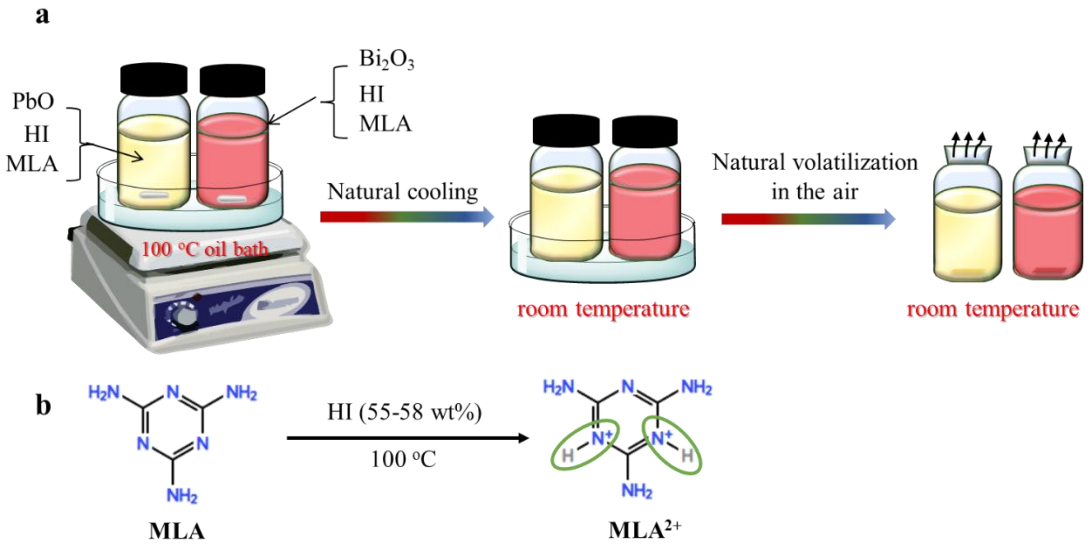

Fig. S1. (a) Synthesis schematic diagram of single crystal of the $(MLA)_2PbI_6{\cdot}2H_2O$ and $(MLA)_2Bi_2I_{10}{\cdot}8H_2O$ SCs. (b) Two *N* atoms in MLA molecule are protonated.

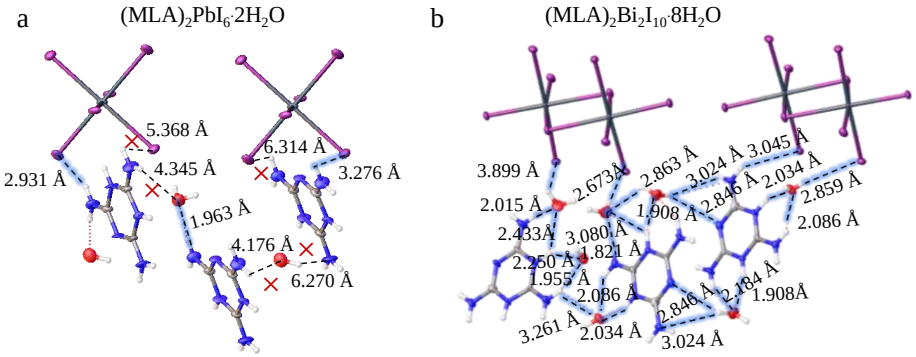

Fig. S2. Hydrogen bonding networks in $(MLA)_2PbI_6{\cdot}2H_2O$ and $(MLA)_2Bi_2I_{10}{\cdot}8H_2O$ SCs, water molecules acting as bridging mediators to strengthen organic ligand interactions.

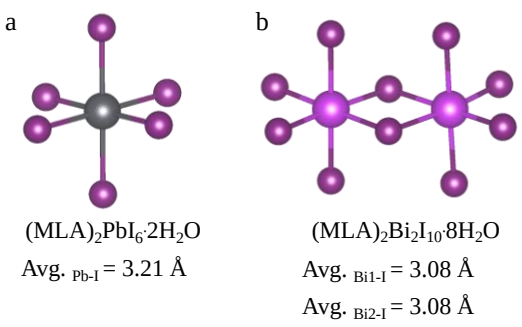

Fig. S3. Average M-I bond lengths of inorganic octahedra of the $(MLA)_2PbI_6{\cdot}2H_2O$ (a) and $(MLA)_2Bi_2I_{10}{\cdot}8H_2O$ (b) SCs.

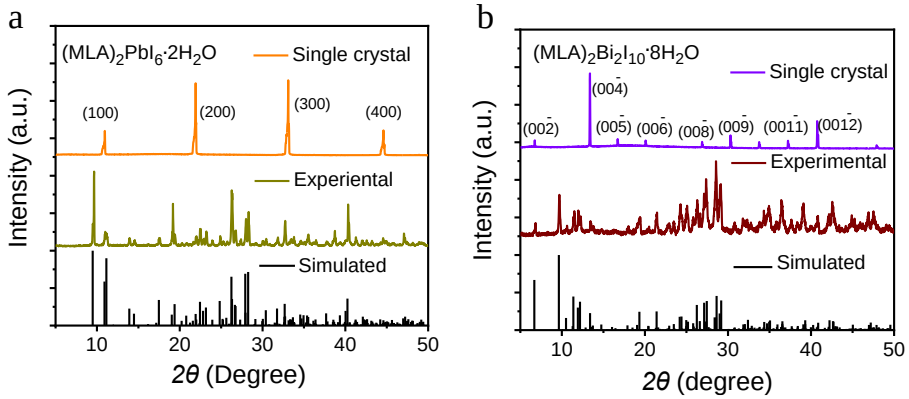

Fig. S4. The XRD patterns of $(MLA)_2PbI_6{\cdot}2H_2O$ and $(MLA)_2Bi_2I_{10}{\cdot}8H_2O$.

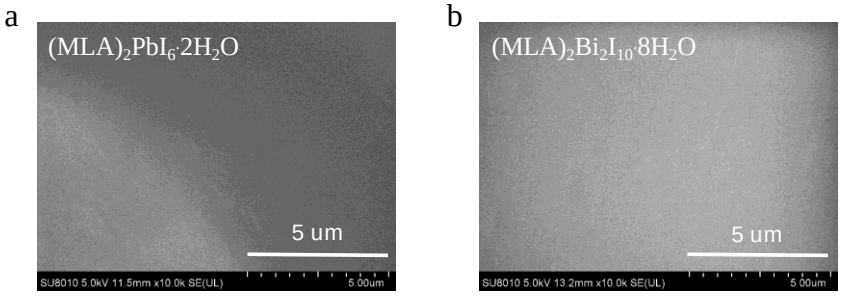

Fig. S5. Top-view SEM images of the $(MLA)_2PbI_6{\cdot}2H_2O$ and $(MLA)_2Bi_2I_{10}{\cdot}8H_2O$ SCs.

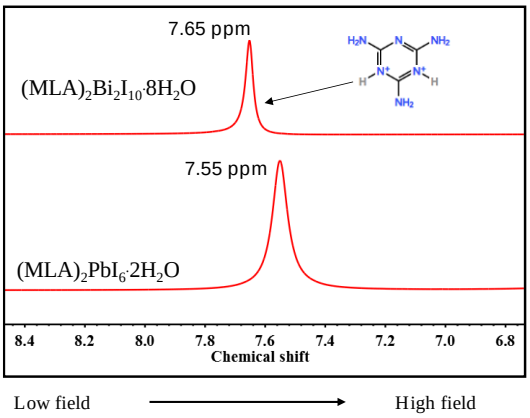

Fig. S6. The ^{1}H-NMR spectra of $(MLA)_2PbI_6{\cdot}2H_2O$ and $(MLA)_2Bi_2I_{10}{\cdot}8H_2O$ dissolved in DMSO-d_6 solvent.

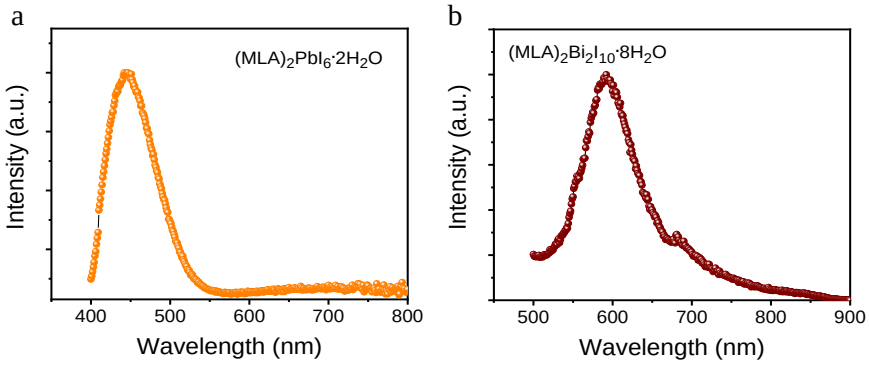

Fig. S7. (a, b) The Photoluminescence spectra of $(MLA)_2PbI_6{\cdot}2H_2O$ and $(MLA)_2Bi_2I_{10}{\cdot}8H_2O$.

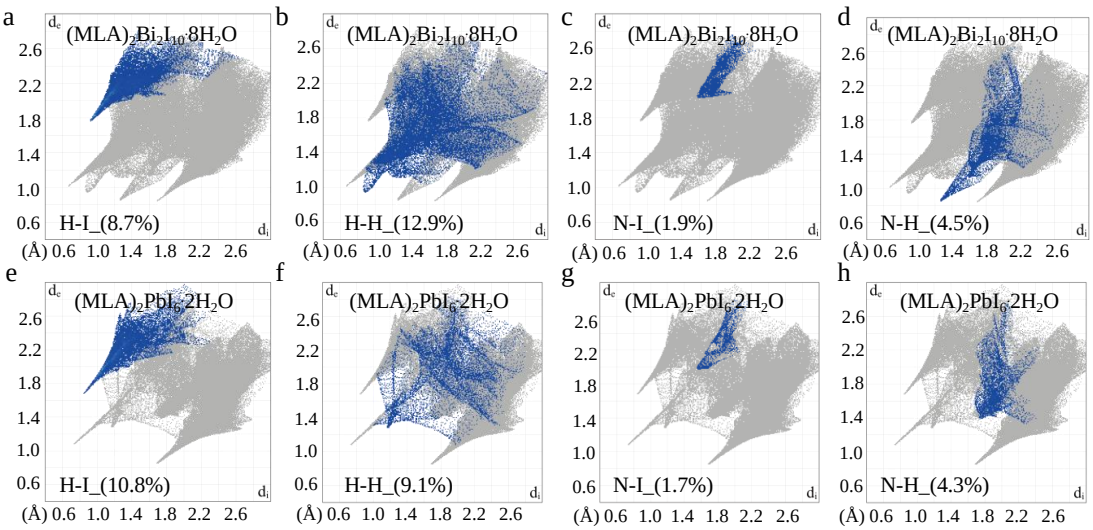

Fig. S8. 2D fingerprint plots of $(MLA)_2PbI_6{\cdot}2H_2O$ (a-d) and $(MLA)_2Bi_2I_{10}{\cdot}8H_2O$ (e-h).

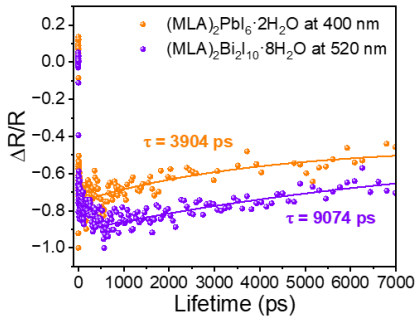

Fig. S9. TR kinetic fit of $(MLA)_2PbI_6{\cdot}2H_2O$ and $(MLA)_2Bi_2I_{10}{\cdot}8H_2O$ SCs recorded at 400 and 520 nm, respectively.

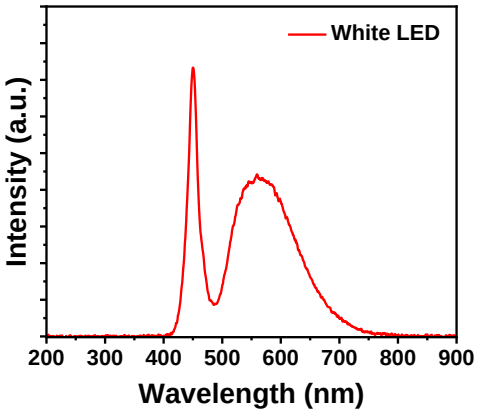

Fig. S10. White LED light wavelength spectrum.

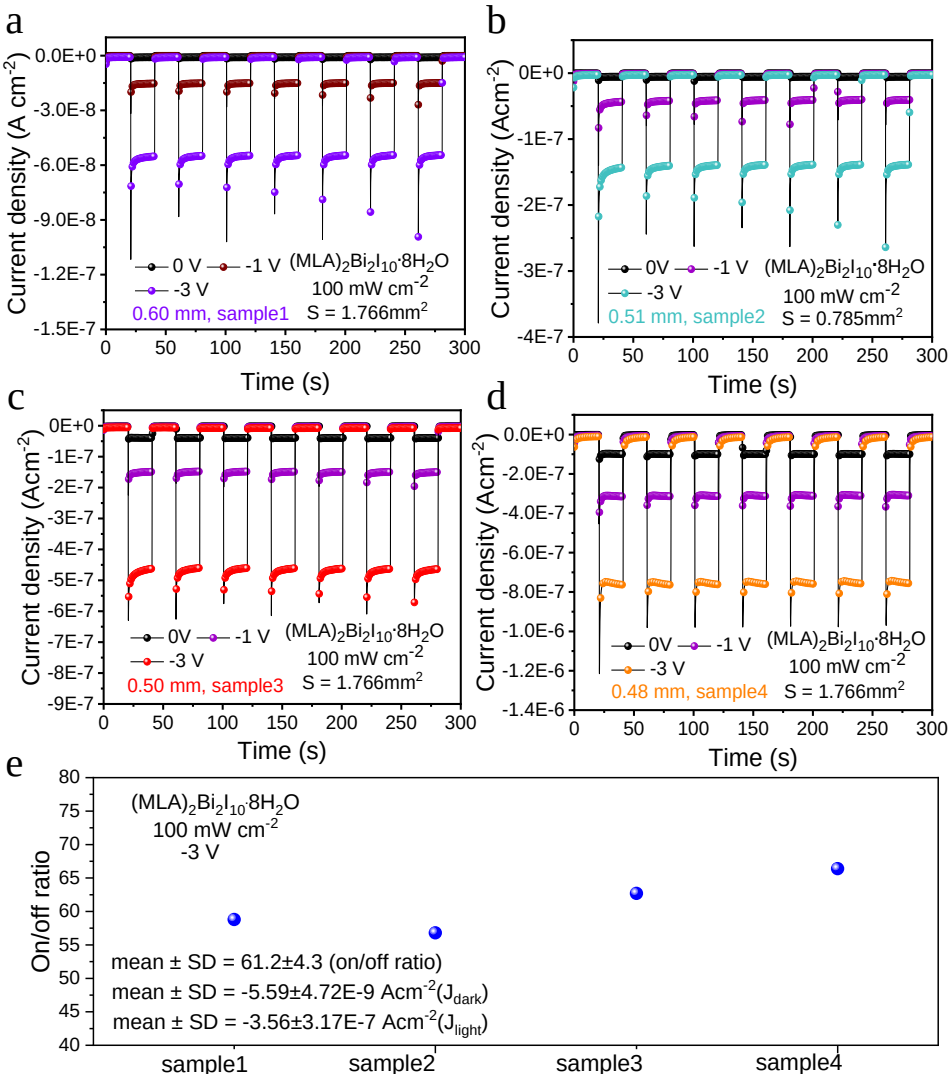

Fig. S11. (a-d) The *i-t* curves of Bi-SC devices at 100 mWcm^{-2}, the illumination wavelength is approximately 400−750 nm. (d) The on/off ratios of different Bi-based devices at −3 V.

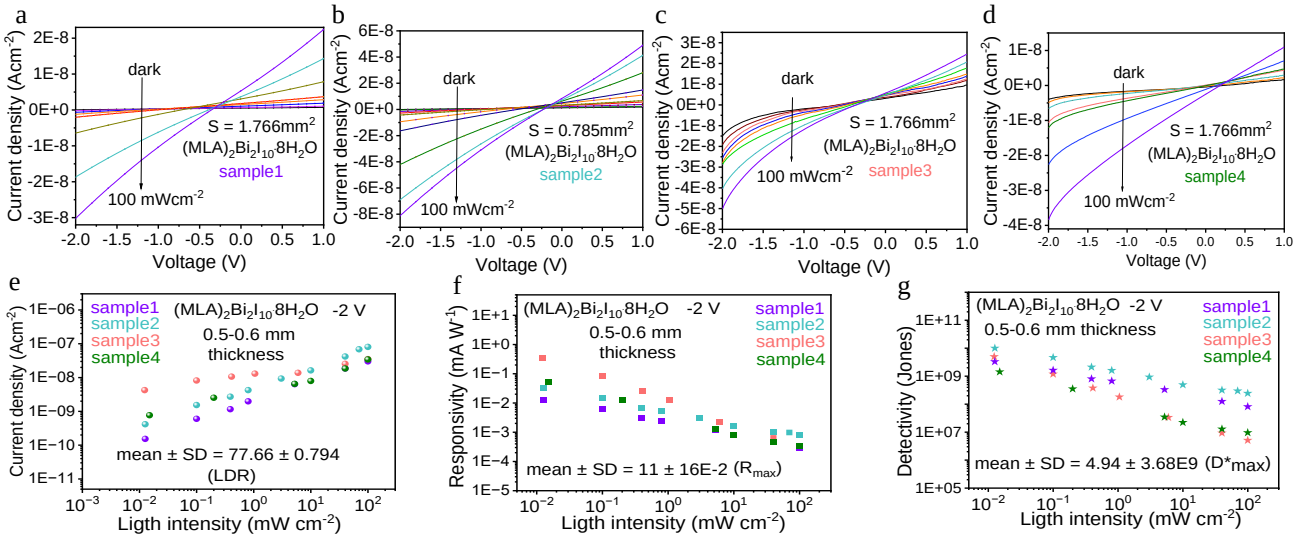

Fig. S12. The *i/v* curves of Bi-SC devices with different batches (a-c). (d-f) Linear dynamic range (*LDR*), responsivity (*R*), and detectivity (*D**) of the Bi-SC device calculated from Fig. S11a-d at −2 V bias under varying light intensities, the illumination wavelength is approximately 400-750 nm.

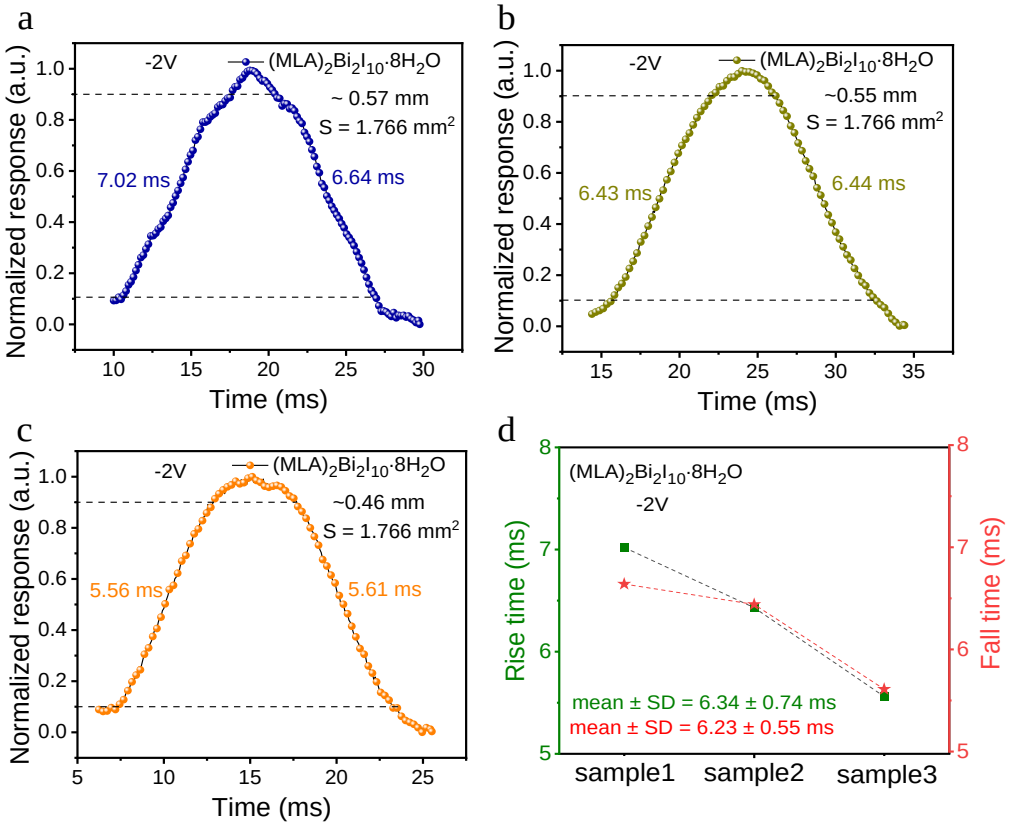

Fig. S13. (a-c) Response time of Bi-SC devices with different thicknesses under a transient white light excitation. Rise time is the time required for the output signal to rise from 10% to 90% of its final stable value, while fall time is the time required for it to fall from 90% to 10% of its stable value after the input signal was removed. (d) The average response time and standard deviation of different devices.

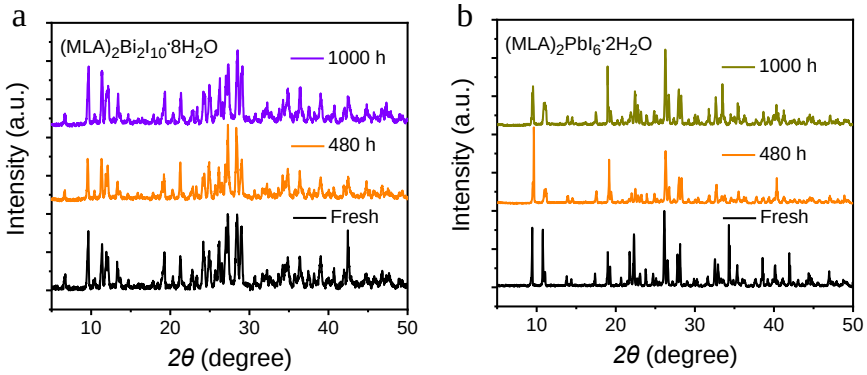

Fig. S14. The humidity stability of $(MLA)_2Bi_2I_{10}·8H_2O$ (a) and $(MLA)_2PbI_6·2H_2O$ (b) powders in air with ~ 55% humidity.

Table S1. Crystal data for the $(MLA)_2PbI_6{\cdot}2H_2O$ and $(MLA)_2Bi_2I_{10}{\cdot}8H_2O$.

Compounds	$(MLA)_2PbI_6{\cdot}2H_2O$	$(MLA)_2Bi_2I_{10}{\cdot}8H_2O$
Empirical formula	$C_6H_{20}I_6N_{12}O_2Pb$	$C_6H_{32}Bi_2I_{10}N_{12}O_8$
crystal system	monoclinic	triclinic
space group	$P2_1/c$	P-1
unit cell dimensions	*a* = 8.32180(10) Å *b* = 18.6369(3) Å *c* = 9.01090(10) Å α = 90° *β* = 103.159(2)° *γ* = 90°	*a* = 8.3908(5) Å *b* = 9.9930(5) Å *c* = 26.7613(12) Å *α* = 95.723(4)° *β* = 94.650(4)° *γ* = 110.042(5)°
volume	1360.83(3)	2081.5(2)
Z	2	2
density (calculated)	3.077	3.330
μ/mm^{-1}	65.730	75.009
index ranges	$-10 \le h \le 10$, $-22 \le k \le 22$, $-10 \le l \le 6$	$-9 \le h \le 10$, $-9 \le k \le 12$, $-33 \le l \le 29$
Independent reflections	2620 [R_{int} = 0.0344, R_{sigma} = 0.0401]	7909 [R_{int} = 0.0618, R_{sigma} = 0.0924]
Data/restraints/parameters	2620/0/128	7909/54/343
Goodness-of-fit on F^2	1.048	0.868
Final R indexes [I>=2σ (I)]	R_1 = 0.0461, wR_2 = 0.1256	R_1 = 0.0427, wR_2 = 0.0775
Largest diff. peak/hole	e $Å^{-3}$ 2.20/-4.63	e $Å^{-3}$ 1.78/-1.49

Table S2. Comparison carrier mobilities and densities of trap state of $(MLA)_2PbI_6{\cdot}2H_2O$ and $(MLA)_2Bi_2I_{10}{\cdot}8H_2O$ single crystals with literature.

Single crystals	n_t (cm^{-3})	μ ($cm^2 V^{-1} s^{-1}$)	*Ref.*
$Cs_3Bi_2I_9$	1.4×10^{10}	/	1
$(BZA)_3BiI_6$	4.25×10^{11}	6.16×10^{-3}	2
$Cs_3Bi_2I_9$	5.7×10^{12}	1.7×10^{-2}	3
$(FA)_3Bi_2I_9$	9.48×10^{9}	8.9×10^{-3}	4
$(MLA)_2PbI_6{\cdot}2H_2O$	3.84×10^{10}	3.29×10^{-4}	This work
$(MLA)_2Bi_2I_{10}{\cdot}8H_2O$	4.30×10^{9}	4.17×10^{-2}	This work

Table S3. Comparison the on/off ratio of $(MLA)_2PbI_6{\cdot}2H_2O$ and $(MLA)_2Bi_2I_{10}{\cdot}8H_2O$ with reported lead-free perovskite single crystals.

Perovskite SCs	Bias voltage (V)	On/Off ratio	*Ref.*
0D $Cs_3Bi_2I_9$	300	> 40	5
0D $(BZA)_3BiI_6$	1	< 2	2
0D $MA_3Sb_2I_9$	5	9	6
0D $GA_3Bi_2I_9$	-	~ 3	7
3D $Cs_2AgBiBr_6$	8	42	8
1D $CsCu_2I_3$	3	31.5	9
1D $(TMHD)BiBr_5$	10	683	10
0D $(MLA)_2Bi_2I_{10}{\cdot}8H_2O$	1	45	This work
0D $(MLA)_2PbI_6{\cdot}2H_2O$	1	3	This work

References

[1] Y. Zhang, Y. Liu, Z. Xu, H. Ye, Z. Yang, J. You, M. Liu, Y. He, M. Kanatzidis, S. Liu, *Nat. Commun.,* 2020, **11**, 2304.

[2] X. Yang, Y. H. Huang, X. D. Wang, W. G. Li, D. B. Kuang, *Angew. Chem. Int. Ed.,* 2022, **61**, e202204663.

[3] W. G. Li, X. D. Wang, J. F. Liao, Y. Jiang, D. B. Kuang, *Adv. Funct. Mater.*, 2020, **30**, 1909701.

[4] W. Li, D. Xin, S. Tie, J. Ren, S. Dong, L. Lei, X. Zheng, Y. Zhao, W. Zhang, *J. Phys. Chem. Lett.*, 2021, **12**, 1778-1785.

[5] Q. Sun, Y. Xu, H. Zhang, B. Xiao, X. Liu, J. Dong, Y. Cheng, B. Zhang, W. Jie, M. Kanatzidis, *J. Mater. Chem. A*, 2018, **6**, 23388-23395.

[6] B. Yang, Y. Li, Y. Tang, X. Mao, C. Luo, M. Wang, W. Deng, K. Han, *J. Phys. Chem. Lett.*, 2018, **9**, 3087-3092.

[7] Y. Xu, J. Hu, X. Xiao, H. He, G. Tong, J. Chen, Y. He, *Inorg. Chem. Front.*, 2022, **9**, 494-500.

[8] Y. Dang, G. Tong, W. Song, Z. Liu, L. Qiu, L. Ono, Y. Qi, *J. Mater. Chem. C*, 2020, **8**, 276-284.

[9] Z. Li, Z. Li, Z. Shi, X. Fang, *Adv. Funct. Mater.*, 2020, **30**, 2002634.

[10] C. Ji, P. Wang, Z. Wu, Z. Sun, L. Li, J. Zhang, W. Hu, M. Hong, J. Luo, *Adv. Funct. Mater.*, 2018, **28**, 1705467.